Metal quantum wells with all electrons confined: Na films and islands on graphite

M. Breitholtz, T. Kihlgren, S.-Å. Lindgren, H. Olin, E. Wahlström, and L. Walldén
Department of Physics and Engineering Physics, Chalmers University of Technology, Göteborg University, SE-412 96 Göteborg, Sweden
(Received 19 April 2001; published 5 July 2001)

Ultrathin Na films and islands on graphite realized prototype simple metal quantum wells with all valence electrons confined within boundaries well defined on the atomic scale. This is shown by angle-resolved photoemission and scanning tunneling microscopy data, which give unique information about electron dispersion, hole lifetimes, and Fermi wavelengths.

DOI: 10.1103/PhysRevB.64.073301 PACS number(s): 73.21.Fg, 68.37.Ef, 79.60.−i

Valence electrons may be confined to a thin metal film even when it is adsorbed on a substrate, which can be a metal or an insulator. One condition is that the electrons have energies within a substrate band gap. Propagation into the substrate is then forbidden and incident electrons are reflected back towards the front side of the film, where the surface potential barrier acts as a second mirror. Multiple reflections between the interfaces sort out standing waves, often referred to as quantum well states (QWS), having perpendicular wave vectors $k_\perp$, given by the phase condition $2k_\perp d+\phi=2\pi m$, where d is the film thickness, ϕ the sum of the phase shifts at the two barriers, and m an integer. The states were first observed by recording I/V characteristics of metal-insulator thin-film sandwiches.[1] More recent work has demonstrated that photoemission, in its angle-resolved version, is an excellent probe of QWS[2–4] down to monolayer thickness.

Apart from providing spectroscopists with new ground for fundamental investigations, the quantized level structure of thin metal films has practical interest since it underlies the giant magnetoresistance phenomenon[5] utilized for reading magnetic memories. More generally QWS spectroscopy attracts interest as a tool that allows atomic scale control of the electronic properties of nanosized objects,[6] this is exemplified by photoemission results for well-ordered Ag films on Fe(100).[7] Most nanosize objects of technical interest are small in more than one direction and photoemission, in combination with scanning tunneling microscopy (STM), is useful, as noted here for Na films and islands on graphite. Particular to Na graphite among the systems studied with photoemission is that, as for an unbacked film, all valence electrons occupy discrete QWS. The reason is that Na valence electrons all occupy states, which have energies E, and parallel wave vectors, $\mathbf{k}_\parallel$, such that any QWS energy band, $E(\mathbf{k}_\parallel)$, runs in a graphite band gap. Along the substrate c axis, $\mathbf{k}_\parallel=\mathbf{0}$, the gap extends 4 eV below E_F, which is well below the band bottom of the Na metal. Away from $\bar{\Gamma}$, the QWS energy increases quadratically with $\mathbf{k}_\parallel$ and reaches E_F without having intersected the upper π band of graphite, which, a short distance from $\bar{\Gamma}$, marks the low-energy limit of the substrate band gap.[8] A semimetal like graphite thus has a band structure such that the Na valence electrons experience boundary conditions similar to those for a film in vacuum or one adsorbed on a substrate with a wide absolute band gap. In previous photoemission studies, semiconductors have provided absolute band gaps, but not wide enough to confine all valence electrons in the metal overlayer. Of further interest is that Na is a prototype simple metal in which valence electrons move as if in a constant potential. If homogeneously thick Na films can be prepared on graphite, these should then be near ideal samples for probing the properties of a confined electron gas with metal density. Here we report on structure and morphological changes of such films as well as on the QWS binding energies, photohole lifetimes, and photoemission cross sections.

As a substrate we use a sample of highly oriented pyrolytic graphite (HOPG) onto which Na is evaporated from a heated glass ampoule broken *in situ*. HOPG consists of azimuthally disordered microcrystals with a common [0001] direction. Photoemission spectra are recorded in the MAX-Synchrotron Radiation Laboratory (Lund University) using *p*-polarized light from a normal incidence monochromator (BL 52) which covers the photon energy range 4–40 eV. All spectra shown are measured along the surface normal such that the bottom states are probed of the free-electronlike energy bands formed by the QWS. We find that near layer-by-layer growth can be obtained in the thickness range tried, 1–15 monolayers (ML), by keeping the substrate at 40 K during deposition followed by annealing (90 K) with approximately one atomic layer added in each cycle [Figs. 1(a) and 1(b)]. The anneal is done either by temporarily reducing the flow of He or passing a current through the sample; the latter procedure is also used to clean the sample by heating it to 1100 K. In the diagrams are indicated the number of atomic layers N, and the quantum numbers m, which are chosen as the number of nodes in the film. The monolayer thus has its nodeless bottom state at $E_b=1.65$ eV and the m=1 state at $E_b=0.17$ eV. As described previously[9] the wave vector at a given energy can be determined via the phase condition and this, together with the measured binding energies, gives the dispersion plotted as points in Fig. 1(c). The straight line shows the dispersion predicted by the free-electron model. Figure 1(d) shows a plot of the emission line width versus the binding energy for lines having an easily determined width. This width is of interest as an upper limit to the width caused by the time it takes for electron-electron and electron-phonon processes to quench the hole left behind by a photoelectron ejected from a well-ordered sample. One line, for 1 ML and $E_b=0.17$ eV, stands out as anomalously wide, but the remaining points fall rather close to a common curve indicating that E_b is of main importance. Aside from binding energy, sample quality, temperature, and experimen-

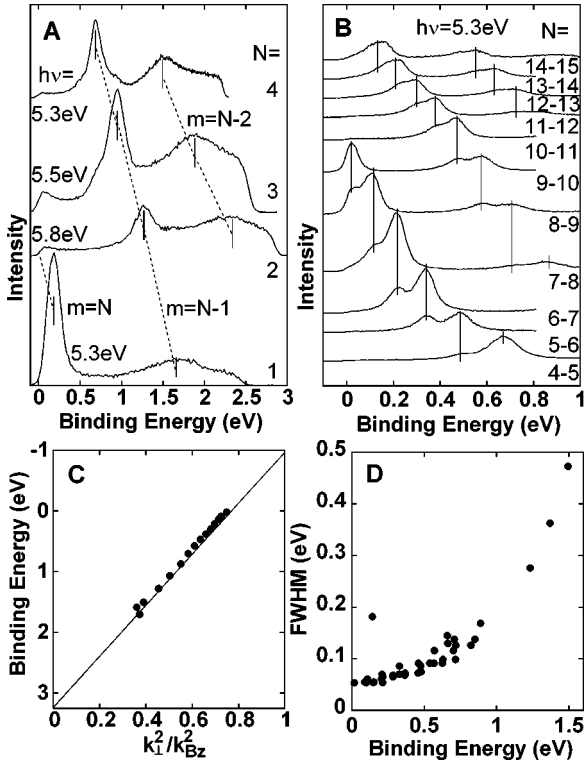

FIG. 1. (a) Photoemission spectra for Na films on graphite. The thickness is given in atomic layers, *N*. Indicated by the spectra are the photon energies hn, and the quantum numbers *m*. (b) QWS emission lines for 4–15-ML-thick Na films on graphite. Doublet emission lines are obtained, since two different thickness values are represented in each spectrum. (c) The dispersion determined for Na metal (points) compared with the free-electron model (straight line). The k values are reduced to the Brillouin zone boundary value $k_{Bz}=\pi/a$, where a is the interplanar distance. (d) The full width at half-maximum (FWHM) of QWS emission lines plotted vs binding energy after subtraction of the contribution due to the experimental resolution (45 meV).

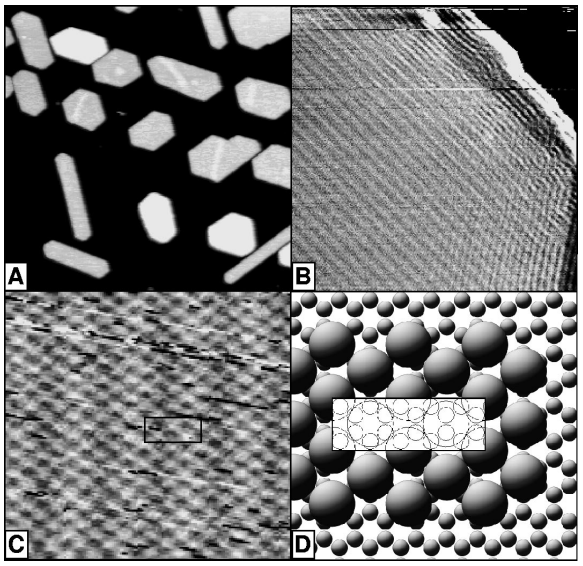

FIG. 2. (a) STM image of 4- and 5-ML-thick Na islands on graphite (70 K, Ubias $=-0.98$ V, $I=42$ pA, 140 nm x 140 nm). (b) Terrace of 5-ML-thick Na island showing the two wavetypes discussed in the text (40 K, Ubias $=-0.011$ V, $I=52$ pA, 23 nm x 23 nm). (c) Buckled Na terrace with atoms resolved (5 ML, 40 K, Ubias = - 0.131 V, $I=69$ pA, 6 nm x 6 nm). (d) Na 110 plane overlaid graphene (small balls circles).

tal resolution, the width of a QWS line is expected to depend on the number of filled QWS that can participate in the decay process and, since a QWS extends with a tail in the substrate, also on the choice of substrate. We are aware of no previous similar data for simple metals or theoretical estimates of hole lifetimes in simple metal quantum wells. In bulk Na, electron-electron decay is estimated to give a width, $\Delta E \approx 0.085 E_b^2$,[10] with energies in eV. This is smaller than obtained here by around a factor of 2 when the experimental resolution has been accounted for.

The anneal temperature has an upper limit near 90 K, above which there is an onset of (3D) growth. For example, if LN_2 is used for cooling (95 K) only a fraction of the substrate surface can be covered with a monolayer before emission lines characteristic of 2 ML are observed. At a somewhat higher temperature the first QWS to appear upon Na deposition are characteristic of 3 ML thickness. If the temperature is allowed to increase, a film breaks up into islands thicker than the film. QWS emission lines indicate that the islands have different but well-defined thickness over large enough surface areas to support states with energies not significantly different from those measured for the films. This is confirmed by images recorded, at 35–80 K, with a variable temperature STM (Omicron GmbH) which show flat, regular-shaped islands with abrupt or terraced edges [Fig. 2(a)]. Typical island sizes vary with temperature during preparation. Lateral extensions vary from a few nm to around 500 nm, while the heights are between 3 and 9 ML. Imaging the islands is quite delicate. An island is sometimes shifted in position or damaged, such that holes are created in an island along with new terraces, or the next image may show two islands where there was previously only one.

Successful STM observations regularly give images with two types of wave pattern in islands with thickness up to 6 ML. Occasionally, also the atomic lattice in a terrace is resolved, and in a few instances, waves as well as lattice are observed in one image [Figs. 2(a)–2(c)]. The lattice matches well with the order in the (110) planes of bcc Na. For one type of wave, the amplitude decays away from edges and imperfections and the wavelength depends on the island height. Fourier transformed images show that there are decaying waves with different wavelengths in one island. More conspicuous in the images is the other wave type, which shows little decay and has a wavelength, of 12.4 ± 0.5 Å, that does not depend noticeably on the island height. The corrugation amplitude (around 0.04 Å at 4 ML thickness) however does. It decreases with increasing thickness, and above 6 ML, no wave is detected. As shown in Fig. 2(b), the wave is often parallel to the edges of a terrace or an island, and sometimes boundaries are observed between areas with different wave directions.

Our interpretation of the STM images is that the Na islands are Na (110) microcrystals having slightly buckled sur-

faces, the height variation detected as the undamped wave. The front of the wave is parallel to the [010] direction and the wavelength, within the limits of experimental error, is equal to the distance between four rows of Na atoms [Fig. 2(c)]. The orientation of the Na layer with respect to the graphene layer is such that, given the lattice parameters of the two solids, a coincidence pattern is obtained. This is schematically shown in Fig. 2(d). If the bcc structure is maintained down to the layer nearest to the substrate, these Na atoms will thus occupy inequivalent sites with different heights above the substrate. This height variation is transferred to the outermost layer but with an amplitude that decays as the thickness is increased such that the wave is observed only for a thickness of 6 ML or less.

Regarding electronic structure the main quantitative information is obtained from photoemission but also the decaying waves observed in the STM as discussed below will be ascribed to QWS. Our photoelectron spectra reveal the full ladder of filled states for 1- and 2-ML-thick films. Two states are filled in each case and for 2 ML a third state extends with a low binding-energy tail into the populated range. The binding energies of these states, or at least their sum, can be understood in simple terms with reference to a two-dimensional (2D) free-electron gas. In this ideal case the filled bandwidth is $n\hbar^2\pi/m$, where n is the surface density of electrons. For 1 and 2 ML Na this gives 1.9 and 3.8 eV, respectively. The thickness of the actual films give space for two partly occupied QWS bands. The 2D values should then be compared with the sums of the observed binding energies, 1.65 eV + 0.17 eV for 1 ML and 2.25 eV + 1.25 eV for 2 ML [Fig. 3(a)]. For thicker films, QWS with energies within 1.7 eV of the Fermi energy are identified.

The dispersion shown in Fig. 1(c) is of interest for a continuing discussion regarding the filled bandwidth in bulk Na metal. Based on a lineshape analysis of photoemission spectra from bulk samples,[11] a band narrowing of around 0.3 eV compared to the free-electron width was deduced,[12] which is in the range predicted by early theory.[13] Recently, however, a widening by the same amount was predicted and also found consistent with the experimental data.[14] The present results show that self-energy corrections must be small (<0.1 eV) in the energy range covered here. In this analysis we have ignored that the bcc structure is perturbed by the misfit to the graphite lattice. Even if the QWS energies are little affected by the lattice distortion this may be significant for the linewidths and explain why the width is particularly large for the thinnest film [Fig. 1(d)]. That structure imperfections are important for the 1 ML film is suggested by the fact that the $E_b = 0.17$ eV state gives a peak width that is three times bigger than for the corresponding state in a Na monolayer on Cu (111).[15] Previously, for Ag/Fe (100), wide QWS emission lines were observed at small thickness, but in that case the substrate has no absolute energy gap, which means that the substrate is not a perfect mirror to incident electrons.[7] A substantial resonant width is then expected at small thickness even if the atomic order at the interface were ideal.

There are two main reasons why a complete ladder of filled states is observed only for 1 and 2 ML thickness. One

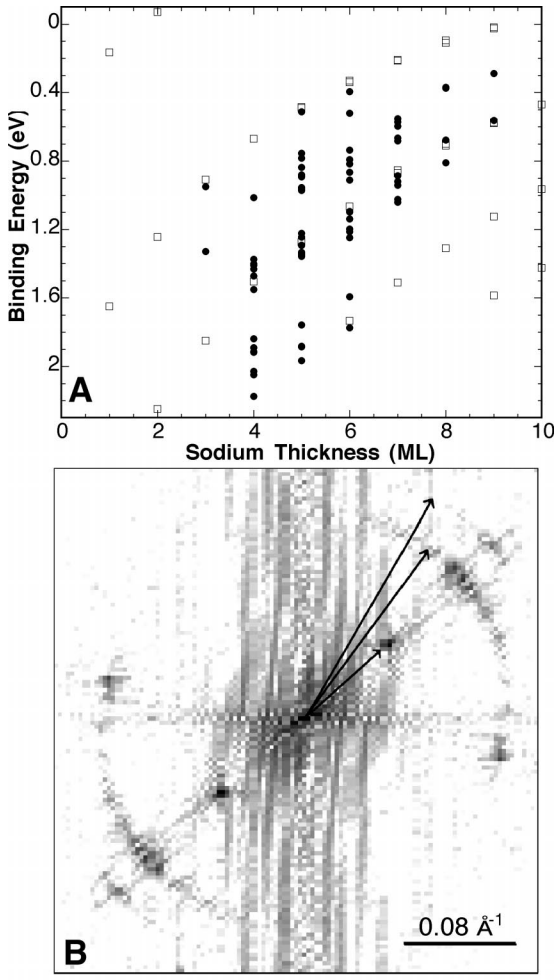

FIG. 3. (a) Thickness dependence of QWS binding energies obtained by photoemission (squares) and binding energies calculated from the Fermi wavelengths measured by STM assuming free-electron dispersion (points). (b) Fourier transform of the image in Fig. 2(b). The two long arrows mark the Fermi contours of two QWS and the short arrow the wave vector characteristic of the buckled surface.

is that the photoemission cross section is large only at photon energies below the plasmon energy (5.7 eV for Na) when the surface barrier induced emission is strong.[16] Using a light source with modest intensity it is then difficult to probe QWS removed from the Fermi level by more than around 2 eV. Even with more intense light another limitation would be met with for 3- or 4-ML-thick films when the level separation between the low-energy states will be smaller than the emission linewidth [Fig. 1(d)]. The integrity of the QWS series is then lost among its low-energy members.

Finally we comment on the decaying waves observed with STM at near zero bias tip-sample bias voltage. Similar decaying waves have been predicted and observed for electrons occupying surface states on (111) surfaces of noble metals.[17–19] As the surface state electrons are scattered by steps between terraces or point defects, there appear lateral standing waves in the electron density sensed by the tip. Considering that only electrons occupying QWS are avail-

able for tunneling at the Fermi level, we interpret the observed decaying standing waves as waves, formed as electrons occupying QWS are scattered against the edges of the islands. To further investigate this assignment, we compare the photoemission data [squares in Fig. 3(a)] with the energies calculated from $\hbar^2k^2/2m$, where k denotes the Fermi wave vectors obtained from Fourier transformed images, and m the free-electron mass [Fig. 3(b)]. It is evident from Fig. 3(a) that standing waves render the same energy dispersion with the number of layers. However, the wavelength of the highest occupied QWS seem to be either shorter than expected, or a mix between the highest and second highest occupied state. We find no obvious explanation for this discrepancy, but note that these states, especially for a metal with low work function, extend with long tails into vacuum, which means that the tip will act as a strong perturbation for these states.

To conclude we have found a preparation procedure for Na covered graphite that gives the opportunity to investigate prototype simple metal quantum wells with all valence electrons confined either to films that can be grown nearly layer-by-layer or to islands with regular lateral shapes and rather uniform heights. STM images show the atomic order expected for a close packed bcc layer and the surface is slightly buckled due to a misfit with the graphite lattice. The dispersion of valence electrons in Na, obtained from the quantized level structure, agrees well with the free-electron model in the upper-half of the filled bandwidth, which is the range that can be easily probed in the present experiment. The results also indicate that even with intense light sources, states much deeper in the well will be difficult to resolve by photoemission. The emission linewidth increases with increasing binding energy while the thickness is less important. This suggests that a photohole is quenched primarily via intraband processes. QWS in Na islands are observed by STM as lateral standing waves near imperfections and boundaries. The wavelengths are in reasonable agreement with the QWS binding energies measured by photoemission except for the longest waves, which have wavelengths shorter than expected.

[1] R. Jaclevic, J. Lambe, M. Mikkor, and W. Vassel, Phys. Rev. Lett. **26**, 88 (1971).

[2] S.-Å. Lindgren and L. Walldén, Solid State Commun. **34**, 671 (1980).

[3] A. Wachs, A. Shapiro, T. Hsieh, and T.-C. Chiang, Phys. Rev. B **33**, 1460 (1986).

[4] T. Miller, A. Samsavar, G. Franklin, and T.-C. Chiang, Phys. Rev. Lett. **61**, 1404 (1988).

[5] M. N. Baibich, J. M. Broto, A. Fert, F. N. V. Dau, F. Petroff, P. Etienne, G. Creuzet, A. Friederich, and J. Chazelas, Phys. Rev. Lett. **61**, 2472 (1988).

[6] F. Himpsel, Science **283**, 1655 (1999).

[7] J. Paggel, T. Miller, and T.-C. Chiang, Science **283**, 1707 (1999).

[8] N. Nishimoto, T. Nakatani, T. Matsushita, S. Imada, H. Daimon, S. Suga, J. Phys.: Condens. Matter **8**, 2715 (1996), and references therein.

[9] S.-Å. Lindgren and L. Walldén, Phys. Rev. Lett. **61**, 2894 (1988).

[10] K. Shung, B. Sernelius, and G. Mahan, Phys. Rev. B **36**, 4499 (1987).

[11] E. Jensen and E. Plummer, Phys. Rev. Lett. **55**, 1912 (1985); I. W. Lyo and E. Plummer, *ibid.* **60**, 1558 (1988).

[12] K. Shung, Phys. Rev. B **44**, R13 112 (1991).

[13] L. Hedin, Phys. Rev. **139**, A769 (1965).

[14] H. Yasuhara, S. Yoshinaga, and M. Higuchi, Phys. Rev. Lett. **83**, 3250 (1999).

[15] A. Carlsson, S.-Å. Lindgren, C. Svensson, and L. Walldén, Phys. Rev. B **50**, 8926 (1994).

[16] P. Feibelman, Prog. Surf. Sci. **12**, 287 (1982).

[17] L. Davis, M. Everson, R. Jaclevic, and W. Shen, Phys. Rev. B **43**, 3821 (1991).

[18] Y. Hasegawa and P. Avouris, Phys. Rev. Lett. **71**, 1071 (1993).

[19] M. Crommie, C. Lutz, and D. Eigler, Nature (London) **363**, 524 (1993).